energies

MDPI

Article

Performance Assessment of R-454C, R-449A, and R-744 in Food Retail Refrigeration Systems †

William Ferretto [1,*], Luca Molinaroli [1] and Fabrizio Codella [2]

[1] Dipartimento di Energia, Politecnico di Milano, 20156 Milano, Italy; luca.molinaroli@polimi.it
[2] Chemours Italy, 20864 Agrate Brianza, Italy; fabrizio.codella@chemours.com
* Correspondence: william.ferretto@polimi.it
† This article is a revised and expanded version of a paper entitled "Energy Efficiency and System Performance of R-454C, R-449A, and R-744 in Food Retail Refrigeration Systems: A Comparison", which was presented at the 8th IIR International Conference on Sustainability and the Cold Chain., Tokyo, June 9–11 2024.

Abstract: Reduced energy use and increased energy efficiency are essential for decarbonization and sustainable development. The food cold chain is a crucial infrastructure with high energy consumption and rising demand. A careful selection of technology used in food retail systems could result in long-term energy savings, functionality, ease of maintenance, and high energy efficiency. In this work, a comparison between the energy performance of three low-GWP refrigerants, namely, R-454C, R-449A, and R-744, is carried out with reference to an existing refrigerating system that serves a real supermarket. Energy usage and seasonal efficiency have been examined for three locations in Europe, representing mild and hot ambient temperatures. Results show that systems based on R-454C and R-449A perform significantly better than R-744 architectures, improving sCOP of up to +12% and +17%, respectively, with a simpler equipment design. This suggests that careful assessment is required to select the most appropriate refrigerant for each store size and climatic condition.

Keywords: commercial refrigeration; low GWP; refrigerants; HFO; CO_2; energy; efficiency

check for updates

Academic Editor: Mahmoud Bourouis

Received: 7 November 2024
Revised: 4 January 2025
Accepted: 14 January 2025
Published: 31 January 2025

Citation: Ferretto, W.; Molinaroli, L.; Codella, F. Performance Assessment of R-454C, R-449A, and R-744 in Food Retail Refrigeration Systems. *Energies* **2025**, *18*, 667. https://doi.org/10.3390/en18030667

Copyright: © 2025 by the authors. Licensee MDPI, Basel, Switzerland. This article is an open access article distributed under the terms and conditions of the Creative Commons Attribution (CC BY) license (https://creativecommons.org/licenses/by/4.0/).

1. Introduction

Greenhouse gas emissions reduction is a compelling worldwide target, as demonstrated by the signing of the Kyoto Protocol [1] and the Paris Agreement [2] by almost all the United Nations countries. Nonetheless, the technological complexity of current applications requires a detailed approach to identify and implement the most effective solutions for decarbonization. In this context, the reduction of energy consumption in the cold chain plays a significant role. It is estimated that 40% of all food requires refrigeration and that 15% of the electricity used globally is for refrigeration [3]. Moreover, up to 60% of the energy used in small- to medium-sized stores is related to refrigeration and food chilling [4]. Therefore, the choice of appropriate refrigeration technology is one of the most relevant measures for energy saving as well as for reduction in the greenhouse gas emission in food stores. In the food cold chain field, three main factors contribute to emissions: direct emissions from food wastes, indirect emissions resulting from the energy generation required by the refrigeration equipment for operation, and direct emissions from refrigerant leaks [5]. Among the three, the indirect effect contributes the most to global warming, accounting for 95% to almost 100% of the total equivalent warming impact (TEWI) of each system [6]. As a result, the environmental measures focusing on energy efficiency gains are more effective than those focused on refrigerant replacement. Supermarket energy usage

varies depending on several factors, including the architecture and size of the store; business and merchandising strategies; and the equipment utilized for on-site food processing, conservation, and display. The refrigerant choice has significant impact on the architecture, energy efficiency, and durability of refrigerating system.

Over the past few decades, the hydrofluorocarbons (HFCs) R-404A, R-507, and R-134a have been chosen as alternatives to chlorofluorocarbons (CFCs) R-12 and R-22, thanks to their null ozone depletion potential (ODP). HFCs have allowed the commercial retail industry to operate in compliance with the Montreal Protocol [7]. Nevertheless, the majority of HFCs are high-Global Warming Potential (GWP) refrigerants. Following the announcements of the Kigali Amendment [8] and the F-Gas Regulation [9] phasing out of high global warming potential (GWP) refrigerants, interest in natural refrigerants, such as carbon dioxide (R-744), and hydrofluoroolefins (HFOs) use increased due to their low GWP.

HFO-based refrigerant blends such as R-454C and R-449A are designed to operate with the same system architecture, components, and maintenance requirements of the older generation of refrigerants. Switching to HFO refrigerants resulted in a significant reduction in energy use for some supermarket chains, which are converting all their property stores to this new technology [10].

R-744, on the other hand, requires additional features to overcome its inherent inefficiencies [11]. As a result, CO_2 cycles differ from traditional, simple layouts, and configurations like booster, mechanical subcooling, and ejector have become the state of the art or are becoming more and more popular.

In the last years, different numerical studies have been conducted to evaluate the performance of different fluids and system configurations and consequently provide indications for the most promising combinations of fluids and system configurations. Citarella et al. [12] numerically evaluated the performance of R-454C, R-449A, R-452A, R-455A, and R-290 as low-GWP substitutes of R-404A for a 2.5 kW commercial refrigeration unit. They performed a thermo-economic optimization at a single operating point. They found that R449A has a slightly higher COP than R-404A (+1%) but provides a lower TEWI (−10% in the Italian scenario), while R-454C, despite its lower COP (−3%), provides the same TEWI reduction as R-449A, which is even higher in the French scenario (−37%). Giménez-Prades et al. [13] evaluated the performance of a supermarket refrigeration system integrated with a subcooling unit operating with R-449A, R-454C, R-290, and new optimized mixtures. They retrieved experimental data for a real supermarket operated with R-449A, from which they developed an empirical model used for the performance evaluation of other fluids. They found that R-454C slightly improves the performance for medium-temperature systems but slightly decreases it for low-temperature systems. Devecioğlu and Oruç [14] evaluated the performance of R-454C, R-455A, R-457A, and R-465A as low-GWP alternatives for R-404A in refrigerators. They developed a simple thermodynamic model, which was used at different evaporating and condensing pressures with the mentioned fluids. They found that R-454C slightly improves the system performance with respect to R-404A but reduces the TEWI by up to 12%. Gullo et al. [15] studied the performance and the environmental impact of eight different configurations operated with R-744 in Athens and Valencia. They used Engineering Equation Solver to model the systems, assuming fixing the temperature differences across the gas cooler. They found that the parallel compression systems provide the same seasonal efficiencies of a R-744/R-134a Cascade System but with a significantly lower environmental impact, up to −25% TEWI. Sun et al. [16] numerically evaluated the performance of a Partial Cascaded Two-stage Compression refrigeration system, operated with R-134a and R-744 in five different climatic zones representative of China. The plant was simulated using a simple thermodynamic approach. They found that the replacement of R-134a with R-744 drastically reduces the system performance at

high ambient temperatures. The addition of a Partial Cascade component can enhance performance, so that the proposed system performance operated with R-744 is comparable with a parallel-booster system operated with R-134a on a seasonal basis. Jeon and Lee [17] evaluated the performance of a R-744-HFC cascade system with R-448A and R-449A as substitute working fluids for R-404A. They developed a thermodynamic model using real compressor operating curves, and they found that R-449A can be used as a replacement for R-404A by adjusting only the refrigerant mass inventory. Moreover, in their study, they highlighted the need for studies on performance comparison of different fluids.

As shown above, few comparisons between different low-GWP HFC and natural fluids have been developed. In this work, the performance of R-449A, R-454C, and R-744 is evaluated when evaluated in state-of-the-art supermarket refrigeration systems. These refrigerants comply with the strictest global rules and regulations as potential alternatives to previous generation high-GWP HFCs. Furthermore, they are today's most common alternatives for designing new commercial refrigeration facilities. However, the determination of the optimal technology solution requires a rigorous process on a case-by-case basis, which should be aided by numerical simulations fed by real components data. To address this need, a numerical model that simulates the steady-state operation of the plant is here developed and presented. Unlike the majority of previous studies, this work employs a semi-analytical approach. Compressors are modeled using data retrieved from manufacturer selection software (BITZER Software v7.04), while high-temperature heat exchangers are simulated using an analytical approach to better capture the fluids' behavior at different ambient temperatures. An existing mid-size retail shop is used as the reference case for simulations, and commercial heat exchanger designs, selected for the supermarket requirements, are incorporated in the model. Seasonal performance indicators are used to assess the refrigerants' performance in three Italian locations, providing insights into their suitability under diverse climatic conditions.

2. Numerical Modeling

This study compares the use of three different refrigerants in a supermarket refrigerating plant: R-454C, R-449A, and R-744. The main properties of the three fluids are evaluated using REFPROP 10.0 [18] and are reported in Table 1.

Table 1. Thermophysical, environmental, and safety characteristics of fluids considered in this work.

Fluid	Composition	T_{CRIT}	P_{CRIT}	NBP [1]	H_{lg} @ −20 °C	ΔT_{GL}@ 15 bar	Molar Mass	GWP	Safety Code
	% By Mass	[°C]	[Bar]	[°C]	[kJ/kg]	[°C]	[g/mol]	100 Years [9]	-
R-454C	R-32: 21.5%, R-1234yf: 78.5%	85.67	43.18	−45.6	206.69	6.91	90.78	146	A2L
R-449A	R-32: 24.3%, R-125: 24.7%, R-1234yf: 25.3%, R-134a: 25.7%	82.07	44.99	−45.99	215.28	4.57	87.21	1396	A1
R-744	R-744: 100%	30.98	73.77	−78.5	282.44	0	44.01	1	A1

[1] Normal Bubble Point.

The goal is to determine whether the state-of-the-art R-744 configuration is competitive in terms of seasonal performance (sCOP) and consumptions with the standard cycle operated with R-454C and R-449A in three Italian cities, namely, Milano, Rome, and Palermo. To simulate the steady-state operation of the machine, a semi-analytical model written in MATLAB^{TM} code is used. The following sections outline the main assumptions and describe the resolution scheme.

2.1. Model Definition

The model follows a bottom–up approach, wherein individual components are modeled separately using their associated sub-model. Subsequently, these component-specific models are integrated to form the system model. The system model follows the procedure outlined below:

1. Refrigerating load calculation;
2. Selection of outdoor air ambient temperature ($T_{AIR,AMB}$);
3. Simulation of the system;
4. Collection of the most relevant data (Q_{EVA}, COP);
5. Reiteration of points 1–4 at different ambient conditions;
6. Data assignment to the annual temperature distribution of the locations under consideration;
7. Calculation of seasonal performance indicators and refrigerant comparison.

2.2. Components Model

2.2.1. Condenser or Gas Cooler

The air-to-refrigerant fin-and-tube heat exchanger is modeled through the elemental volume approach. The model requires the division of the heat exchanger into small elemental volumes and the solution of mass, momentum, and energy balances on each volume. Each elemental volume consists of refrigerant stream, single tube, fins, and air stream, as shown in Figure 1, and is considered as a crossflow heat exchanger, with air as the unmixed stream and refrigerant as the mixed one.

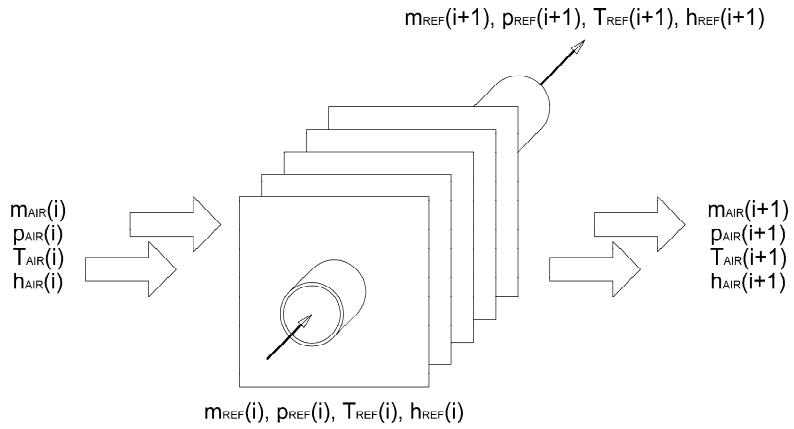

Figure 1. Schematic of a generic elemental volume.

The heat transfer on an elemental volume is accounted for using the ε-NTU method, as in Equations (1)–(4). A more detailed explanation of the heat transfer model, omitted here for the sake of brevity, is found in previous works by the authors [19,20]. The thermal power exchanged on a generic elemental volume is:

$$\dot{Q}_i = \varepsilon_i \cdot C_{MIN,i} \cdot (T_{REF,IN,i} - T_{AIR,IN,i}) \quad (1)$$

where the effectiveness ε_i is computed according to:

$$\varepsilon_i = \begin{cases} \frac{1-\exp[-C_R\cdot(1-\exp[-NTU])]}{C_R} \rightarrow \text{if } (\dot{m}c_P)_{MIN,i} = (\dot{m}c_P)_{AIR,i} \\ 1-\exp\left[-\frac{1-\exp[-NTU\cdot C_R]}{C_R}\right] \rightarrow \text{if } (\dot{m}c_P)_{MIN,i} = (\dot{m}c_P)_{REF,i} \\ 1-\exp(-NTU) \rightarrow \text{if two-phase flow} \end{cases} \quad (2)$$

and the capacity ratio C_R and the number of transfer units NTU as:

$$C_R = \frac{C_{MIN}}{C_{MAX}} \tag{3}$$

$$NTU = \frac{UA}{C_{MIN}} = \frac{(R_{REF} + R_K + R_{AIR})^{-1}}{C_{MIN}} \tag{4}$$

The refrigerant side heat transfer resistance in Equation (4) and pressure drop are computed through the correlations summarized in Table 2. The air side heat transfer coefficient and pressure drop are computed according to the Wang model [21]. All the correlations were chosen so that the actual case study would fall in the correlations range of validity. On the calculation of the heat transfer coefficient in two-phase conditions with mixtures, the Bell and Ghali [22] correction is applied.

Table 2. Refrigerant heat transfer coefficient and pressure drop correlations.

	Single-Phase	**Two-Phase**	**Transcritical**
Heat transfer	Gnielinski [23]	Cavallini [24]	Gnielinski
Pressure drop	Blasius [25]	Quibén [26]	Blasius

The air flow rate on the gas cooler/condenser is computed to satisfy the fluid dynamic match between the heat exchanger and the fan characteristic curves.

2.2.2. Expansion Valve

The expansion process is considered to be isenthalpic. To operate properly, expansion valves require a minimum pressure difference of 2.5 bar: the condensing pressure is consequently set to satisfy the requirements. In subcritical cycles, the expansion valves are supposed to be able to guarantee the superheat at the evaporator outlet, whatever the operating conditions are, whereas in the transcritical cycle, the expansion valve at the gas cooler outlet operates as back pressure and is supposed to adjust the high-pressure side to maximize the COP.

2.2.3. Evaporator and Cooling Load

The evaporators are modeled using the energy balance:

$$\dot{m}_{REF,EVA} = \frac{\dot{Q}_{EVA}}{(h_{OUT,EVA} - h_{IN,EVA})} \tag{5}$$

The cooling load is provided by the case study specifics and is kept constant at the different environmental conditions considered. The inlet conditions depend on the plant specifics, while the outlet conditions are retrieved as follows:

$$h_{OUT,EVA} = h(\min(P_{EVA}), \min(T_{EVA} + \Delta T_{SH})) \tag{6}$$

Usually, the duty is grouped together according to the evaporating temperature, forming medium-temperature (MT) or low-temperature (LT) sections. Hence, for each refrigerating section, the required mass flow rate, the inlet, and outlet refrigerant enthalpies are computed accordingly.

2.2.4. Internal Heat Exchanger (IHX)

The internal heat exchangers, which may be present in the plant, are modeled through an energy balance. In this study, only Liquid Line–Suction Line Heat Exchangers (LL-

SLHXs) are considered as IHXs. On the hot liquid and cold vapor sides of the heat exchanger, the mass flow rate is equal, while the heat capacity is higher on the liquid side. It is assumed that the vapor side undergoes a heating process, which raises the refrigerant temperature by 5 K, while the liquid cools down according to the energy balance.

If the liquid inlet temperature is lower than the outlet vapor temperature incremented by a temperature approach, the LL-SLHX is bypassed. This condition may be encountered at very low ambient temperatures, in which the condenser outlet temperature is low and may be similar to the outlet temperature of the loads at the highest evaporating temperature.

2.2.5. Compressor

Polynomial curves supplied by the manufacturer are used to simulate the compressor. The polynomial curves provide the refrigerant mass flow rate and input electric power as a function of the condensing and evaporating temperatures (or evaporating temperature and discharge pressure for transcritical operation). As the compression process, it is assumed to be adiabatic; the outlet refrigerant conditions can be determined through the following energy balance:

$$\dot{W}_C(P_{EVA}, P_{COND}) = \dot{m}_C(P_{EVA}, P_{COND}) \cdot [h_{R,OUT}(T_{R,OUT}, P_{COND}) - h_{R,IN}(T_{R,IN}, P_{EVA})] \quad (7)$$

To satisfy the requested mass flow rate computed as per Section 2.2.3, an appropriate number of compressors, one of which is an inverter-driven compressor, is chosen.

2.3. System Layouts and Resolution Algorithms

Two different layouts have been studied for R-454C and R-449A, while a single, more complex layout is analyzed for R-744.

2.3.1. Basic Layout for R-454C and R-449A

The most used design for commercial refrigeration systems is the basic vapor compression cycle (VCC) based on R-404A technology, which is valued for its simplicity, robustness, and ease of maintenance. R-454C and R-449A are meant to be utilized in such systems as drop-in, re-modeling, or completely new installations. The standard configuration constitutes four basic components of a VCC: compressor, condenser, expansion valve, and evaporator (Figure 2). The plant is solved according to the resolution scheme in Figure 3a, in which it is worth mentioning the evaporating temperature is set by the application (MT or LT) and kept constant throughout the entire simulation.

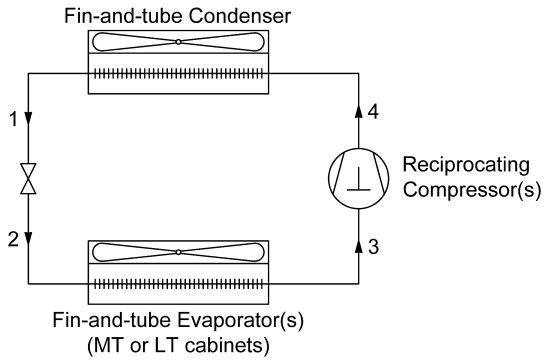

Figure 2. Basic VCC system layout.

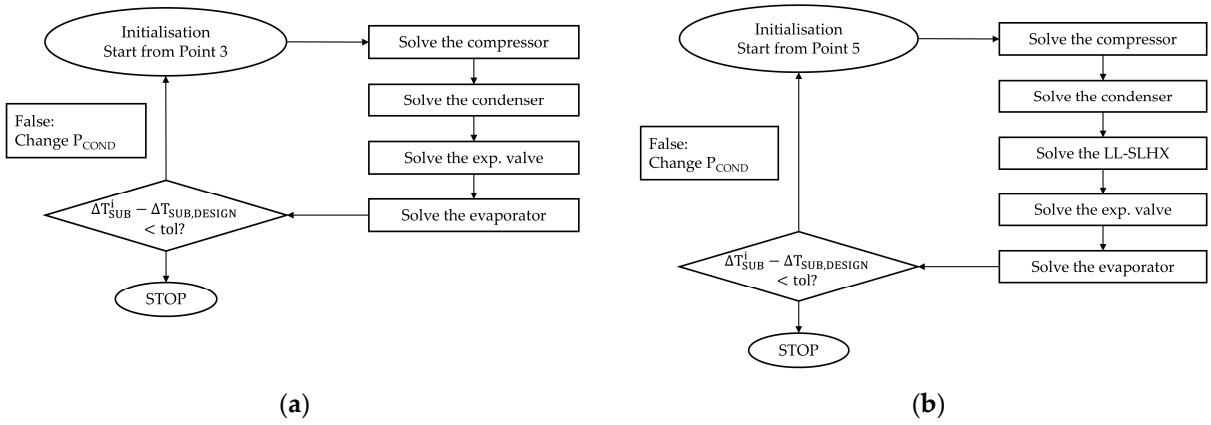

(**a**) (**b**)

Figure 3. (**a**) Resolution scheme for basic VCC. (**b**) Resolution scheme for LL-SLHX basic VCC and subcritical CO_2.

2.3.2. LL-SLHX Layout for R-454C and R-449A

A second configuration for R-454C and R-449A comprising Liquid Line—Suction Line Heat Exchanger (LL-SLHX) is presented in Figure 4. The plant is solved according to the algorithm presented in Figure 3b.

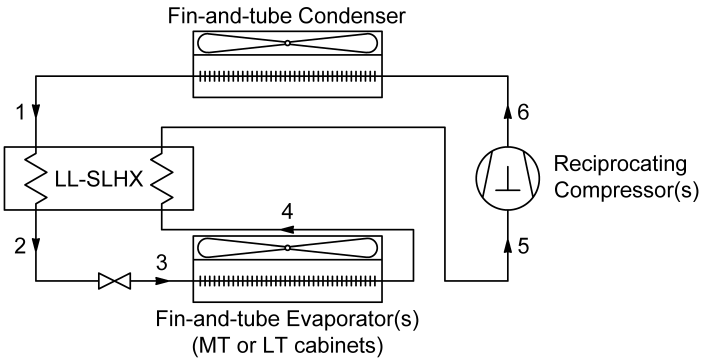

Figure 4. System layout with internal heat exchanger.

2.3.3. System Layout: R-744

An advanced state-of-the-art system layout for R-744 is considered, comprising parallel compression, flash gas bypass, and liquid line–suction line internal heat exchanger, as shown in Figure 5.

The R-744 system is designed to operate in two modes, subcritical and transcritical, according to the ambient air temperature: subcritical operation if $T_{AIR,AMB} < 20$ °C, transcritical operation if $T_{AIR,AMB} \geq 20$ °C.

In subcritical operation, the back pressure valve (1–2) is completely opened, and the flash tank does not produce any flash gas since it operates as a liquid receiver.

During transcritical operation, the flash tank generates flash gas, which flows through either the flash gas valve or the parallel compressor. It is important to note that the dynamic behavior of the system is not captured due to the steady-state nature of the model. Consequently, this study focuses on the configuration with the parallel compressor and the flash tank set to 36 bar. The parallel compressor is an inverter-type compressor, with a frequency chosen to manage all the flash gas produced. The gas cooler operating pressure is chosen to optimize the refrigerating system's COP. Several correlations are available in the literature, depending on the system configuration. The most representative one for this equipment is Sawalha [27]:

$$P_{GC} = 2.7 \cdot (T_{AIR,AMB} + \Delta T_{APP}) - 6.1[bar] \quad (8)$$

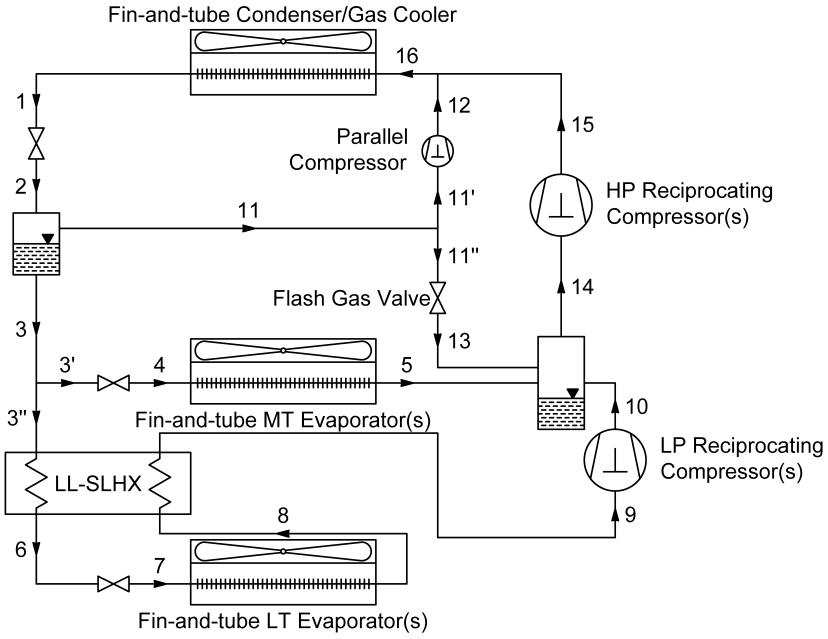

Figure 5. R-744 system layout.

The value of ΔT_{APP} is assumed to be a constant equal to 2 K. If the correlation indicates subcritical pressure while the air temperature is above 20 °C, the operating pressure is set to 80 bar.

The system is solved according to the scheme reported in Figure 6 if the operation is transcritical, while the scheme in Figure 3b is used if the operation is subcritical.

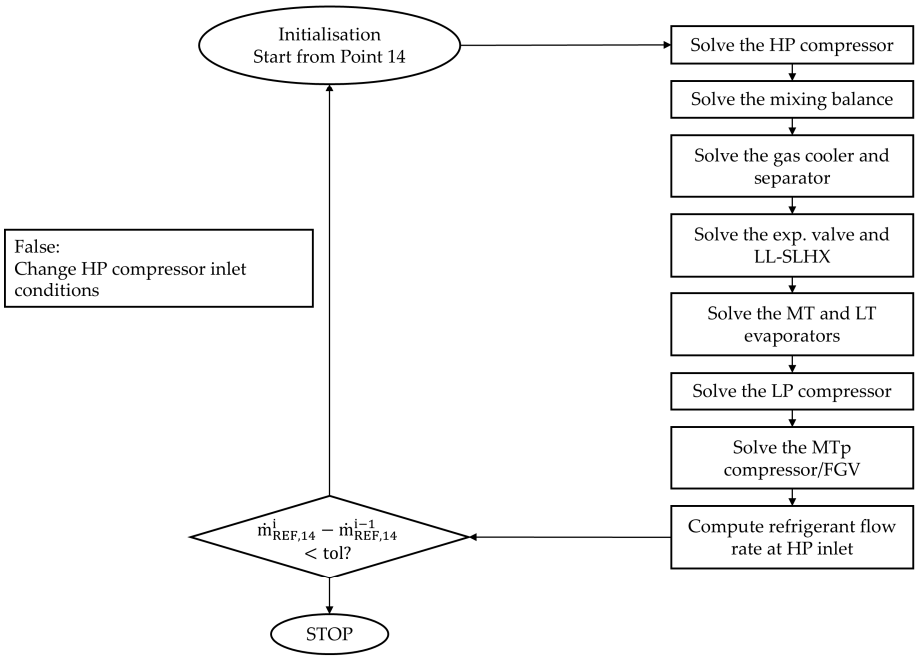

Figure 6. Resolution scheme for transcritical operating R-744.

3. Case Study

An existing facility is chosen to delineate the store layout and determine the configurations of the refrigeration systems, along with the corresponding cooling loads. The different cooling loads according to the evaporating temperature are reported in Table 3.

Table 3. Cooling loads and operating temperatures.

Cooling Section	Evaporating Temperature [°C]	Load [kW]
MT1	−2	31.88
MT2	−10	33.50
LT	−35	27.42
TOT		92.80

According to the operating fluid and layout, the sections are managed differently, as explained in the following section.

3.1. Assumptions

The HFO refrigerant blends R-454C and R-449A operate with an identical system configuration, as shown in Section 2. Each cooling section (MT1, MT2, and LT) has a dedicated condenser. On the other hand, the R-744 system manages the MT1, MT2, and LT sections simultaneously, and is equipped with a single condenser/gas cooler to optimize the high costs of R-744-specific components. Based on the store layout, the general assumptions in Table 4 have been made.

Table 4. System layouts general assumptions.

Variable	Value	Unit
Discharge line length	20	m
Suction line length	20	m
Liquid velocity	<0.5	m/s
High-pressure line thermal loss	0	K
Low-pressure line non-useful ΔT_{SH}	10	K
Evaporator Outlet useful superheat	5	K
Internal Heat Exchanger $\Delta T_{6\text{-}1}$	5	K
Internal Heat Exchanger ΔT_{APP}	2	K
Gas Cooler ΔT_{APP}	2	K
Condenser Outlet subcooling	$f(T_{AIR,AMB})$ [1]	K
Fans Speed	$f(T_{AIR,AMB})$ [1]	rpm

[1] As per Table 5.

The liquid velocity value is used to size the liquid discharge line diameter. The suction line diameter is sized to limit the pressure drop to 1.5 K (saturation temperature). Since the values of the two resulting diameters are similar, a single value, corresponding to that of the liquid line, is used. Pressure drop in the two lines is computed according to the Blasius model [25].

The subcooling of the refrigerant and the rotational speed of fans are a function of the ambient air temperature at the condenser/gas cooler inlet, as reported in Table 5.

The systems are simulated for a set of outdoor air temperatures ranging from −5 °C to +40 °C.

Table 5. Subcooling and fan rotational speed as a function of air ambient temperature.

T_{AMB} [°C]	ΔT_{SUB} [°C]	N [rpm]
[−5;0)	8	N_{MIN}
[0;5)	6	
[5;10)	4	
[10;20)	3	
[20;30)	2 [1]	$N_{MIN} + (T_{AIR,AMB} - 20)/10 \times (N_{MAX} - N_{MIN})$
[30;40)	2 [1]	N_{MAX}

[1] Only for R-454C and R-449A systems.

3.2. Results Reduction

Since the plants operating with R-449A and R-454C provide the requested load by three different sub-plants (i.e., MT1, MT2, and LT), the COP, sCOP, and energy consumption are computed by aggregating the thermal loads and the corresponding consumptions. The sCOP and yearly energy consumption are calculated according to:

$$\mathrm{sCOP} = \frac{\sum_{i=1}^{8760} \dot{Q}_{EVA,i}}{\sum_{i=1}^{8760} \dot{W}_C(T(o_i))} \tag{9}$$

$$W_{TOT} = \sum_{i=1}^{8760} \dot{W}_C(T(o_i)) \tag{10}$$

The year hourly distribution of the outdoor air temperature in the selected locations is retrieved from METAR data. Milano (MI), 45°28′ N; Rome (RO), 41°53′ N; and Palermo (PA), 38°6′ N are chosen to represent the moderate, moderate–hot, and hot climates of Italy, since the climate of Palermo is similar to the reference European hot climate (Athens). Figure 7 shows the temperature distributions over the last 10 years (2013–2023) of the three selected cities.

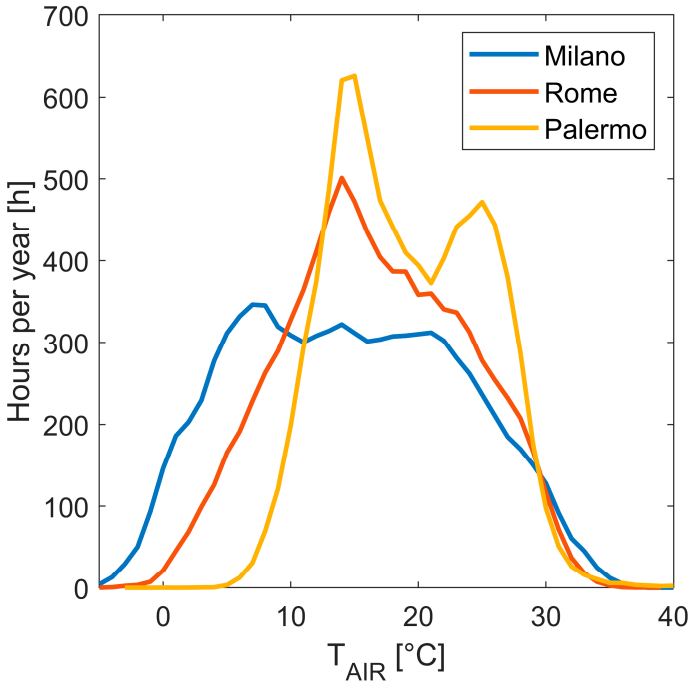

Figure 7. Yearly number of hours of outdoor air temperature in Milano, Rome, and Palermo.

4. Results and Discussion

The findings of this study are analyzed from two points of view. The first focuses on the behavior of the plant efficiency as a function of the outdoor ambient temperature. The second focuses on the seasonal efficiency and energy consumption of all the plants.

4.1. Comparison of Synthetic Refrigerants

In this section, R-449A and R-454C are first compared in terms of the number of compressors required to meet the refrigeration load in each analyzed city. Particularly, Table 6 shows the annual distribution of operating hours for the required number of compressors operated with synthetic refrigerants, in both simple and LL-SLHX configurations.

Table 6. Number of compressors required and yearly work-hour distribution for R-449A and R-454C used in all the plant configurations: Milano (MI), Rome (RO), and Palermo (PA).

Fluid	Load Level	MI Number of Compressors			RO Number of Compressors			PA Number of Compressors		
		1	2	3	1	2	3	1	2	3
R-449A Base	MT1	4437	4323	-	3575	5185	-	2215	6545	-
	MT2	-	7440	1320	-	7368	1392	-	6779	1981
	LT	2884	5876	-	1511	7249	-	239	8516	5
R-454C Base	MT1	1231	7529	-	374	8386	-	-	8757	3
	MT2	-	4405	4355	-	3575	5185	-	1594	7166
	LT	1231	7510	19	374	8381	5	-	8727	33
R-449A LL-SLHX	MT1	4437	4323	-	3575	5185	-	2215	6545	-
	MT2	-	8389	369	-	8506	254		8537	223
	LT	4437	4323	-	3575	5185	-	2215	6545	-
R-454C LL-SLHX	MT1	1231	7529	-	374	8386	-	-	8760	-
	MT2	-	6283	2477	-	6017	2743	-	5108	3652
	LT	2886	5874	-	1511	7249	-	238	8517	5

R-454C requires more working hours with a higher number of compressors than R-449A, and specifically, it requires more compressors for LT load in Milano and Rome. This is caused by the lower phase-change enthalpy of R-454C compared to R-449A, as described in Table 1. Since the cooling load is fixed to the same value for all refrigerants, this leads to a higher mass flow rate and, consequently, higher displacement required. The relative distance between the two fluids is almost identical when comparing the three cities, suggesting that both fluids have similar performance behavior with ambient temperature.

The use of a LL-SLHX reduces the evaporator inlet enthalpy, consequently reducing the required mass flow rate, hence the compressor burden. Indeed, it should be highlighted that for MT2 and LT loads of both fluids, most of the cooling load is satisfied with a lower number of compressors compared to the simple layout case. Particularly, the use of a LL-SLHX allows R-454C in the LT load to operate in Milano and Rome with one compressor less than the simple layout case. On the other hand, the hour distribution for the MT1 load of both fluids is equal between the LL-SLHX and simple layout. In the MT1 load, the evaporating temperature is higher, and consequently, the LL-SLHX subcooling effect is lower. Moreover, the MT1 inverter-driven compressor works well above the minimum frequency 25 Hz, hence the mass flow rate reduction is handled without changes in the hour distribution.

R-449A and R-454C are then analyzed in terms of the operative compression ratios. Figure 8 shows the behavior of the compression ratios of R-449A and R-454C in MT1 and LT loads in the simple layout configuration. The behavior of the MT2 load follows very closely the MT1 behavior, while the IHX configuration almost overlaps the corresponding lines; hence, for the sake of graphic simplicity, they are omitted from the figure.

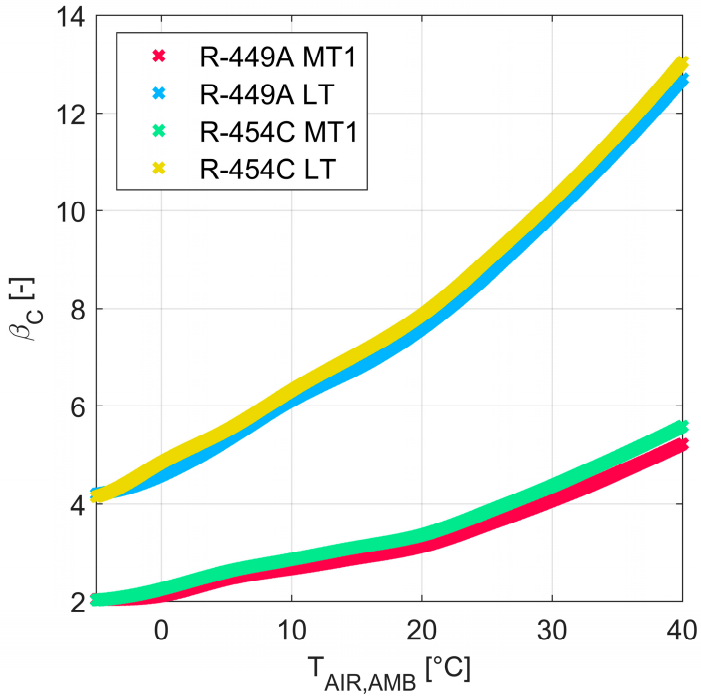

Figure 8. Behavior of compression ratio with ambient temperature for R-449A and R-454C operated in MT1 and LT cooling loads.

R-454C requires a higher compression ratio than R-449A in all configurations and ambient temperatures analyzed. As described in Section 2, the resolution algorithm changes the condensing pressure and temperature to meet the required subcooling, given the same heat exchanger design used for both fluids. Since R-454C requires a higher compression power than R-449A, the power to be rejected through the condenser is higher. Moreover, since R-454C has a higher glide temperature than R-449A, the heat transfer coefficient is further penalized [22]. In view of these two phenomena, it is necessary to increase the R-454C saturation temperature to satisfy the subcooling requirements. This translates into lower compressor volumetric and isentropic efficiencies, which in turn reduce the system efficiency. If the heat exchanger had a higher heat transfer area, the simulations would have shown the result overturned since, given two temperature levels, R-454C has a lower compression ratio than R-449A. This demonstrates that an analytical simulation of the heat exchangers is required when analyzing the system performance to accurately capture all the phenomena arising from the different thermophysical properties of working fluids.

4.2. COP Behavior with Outdoor Ambient Temperature

The COP for the three refrigerants as a function of outdoor air temperature is represented in Figure 9 with reference to a base layout configuration (a) and to the LL-SLHX configuration (b).

R-454C and R-449A operating plants exhibit a similar pattern of gradual performance reduction as the outdoor temperatures increase, with R-449A performing better than R-454C in all operating temperatures. On the other hand, R-744 plant shows good performance at outdoor temperatures below 20 °C when it operates in subcritical mode, but it experiences a significant drop in energy efficiency at outdoor temperatures above 20 °C, correspondent to transcritical mode operation. If the basic VCC is considered (Figure 9a), the R-744 system outperforms both synthetic blends in terms of COP only when the outside temperature is below 15 °C, highlighting its higher sensitivity to temperature variation. The presence in the R-744 operating plant of a LL-SLHX allows for a lower inlet enthalpy in the LT evaporator and, consequently, a lower requested refrigerant flow rate. This contributes to a reduction in LT compression power and, hence, to a higher COP in the subcritical mode.

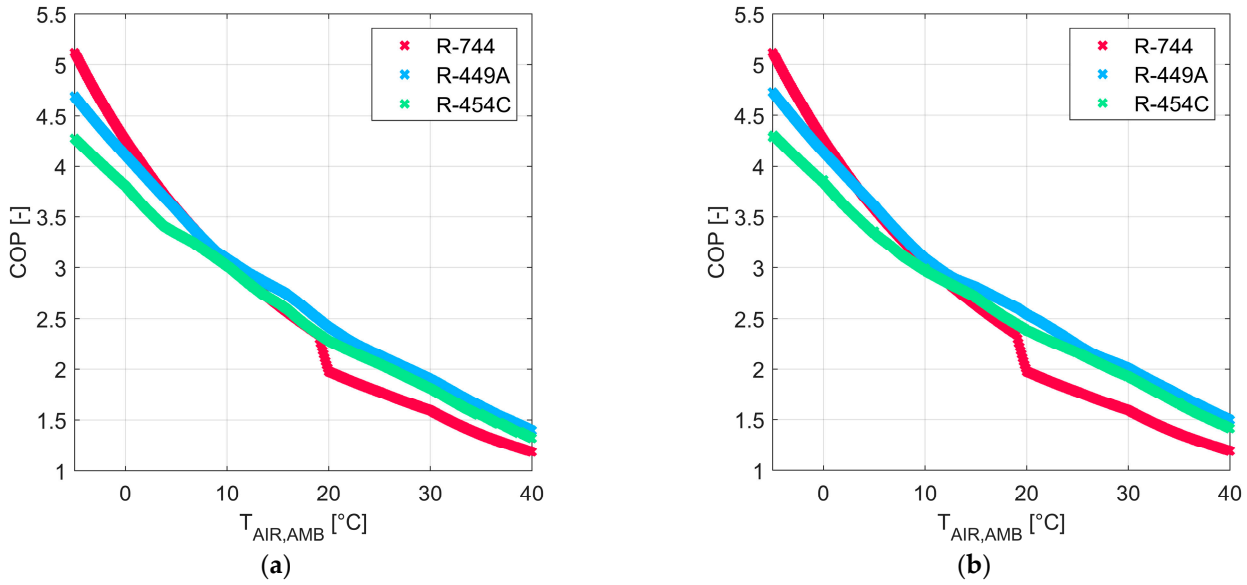

Figure 9. Cooling COP behavior with outdoor ambient temperature for (**a**) R-449A and R-454C operating with basic VCC and R-744, and (**b**) R-449A and R-454C operating with LL-SLHX VCC and R-744.

The use of the LL-SLHX in the R-454C and R-449A VCC plants provides an improvement, which is clearly visible in Figure 9b. The improvement is limited at low temperatures, on average +0.7% at −5 °C, but significant at high temperatures: the performance at +40 °C is improved by +6.7% and +7.0% for R-454C and R-449A, respectively. From a COP point of view, the employment of an IHX significantly reduces the working range of R-744 plants in favor of synthetic refrigerants.

4.3. Seasonal Results

The results are reported in terms of seasonal COP and energy consumption in Table 7, while Figure 10 shows the sCOP percentage difference of R-449A and R-454C from R-744, which is considered the baseline case, evaluated in each city.

The results show that the R-744 plant has a significantly lower performance with respect to R-454C and R-449A. When R-449A and R-454C LL-SLHX plants are operated in the hottest city, i.e., Palermo, the difference with respect to R-744 is 17% and 12%, respectively. The hotter climate of the southern part of Italy greatly favors the use of synthetic refrigerants plants, while CO_2 suffers the high-pressure transcritical operation. In Rome and Milano, the difference takes a lower value owing to the colder temperature distribution but, nevertheless, remains significant, especially if R-449A is used as the operating fluid. Moreover, moving from Milano to Palermo, R-744 is the most sensitive to the temperature

change, with a −12.5% sCOP change, while the other two fluids stay around −9−−10% sCOP variation, confirming the worse behavior of R-744 at high ambient temperatures.

Table 7. sCOP and energy consumption of the configurations analyzed in Milano (MI), Rome (RO), and Palermo (PA).

Configuration and Fluid	sCOP [-]			Energy Consumption [MWh]		
	MI	RO	PA	MI	RO	PA
R-449A Base	2.72	2.61	2.46	298.65	312.04	331.05
R-454C Base	2.59	2.48	2.34	313.86	327.16	347.03
R-449A LL-SLHX	2.80	2.68	2.54	290.53	303.38	320.57
R-454C LL-SLHX	2.66	2.56	2.43	305.56	317.76	334.81
R-744	2.48	2.35	2.17	328.00	346.33	374.93

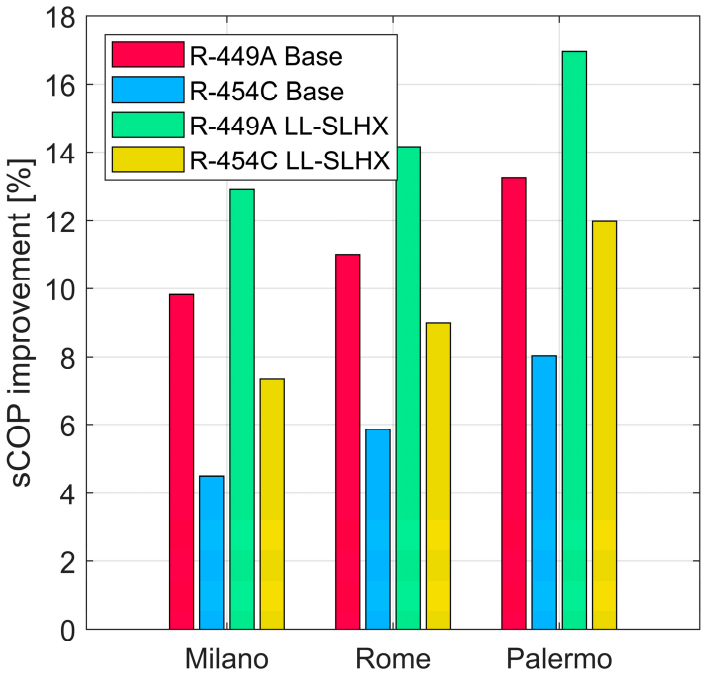

Figure 10. sCOP difference of the plants operating with R-454C and R-449A with respect to R-744 plant, evaluated in each city.

The insertion of an IHX in basic VCC cycles is appreciable also from the point of view of sCOP, as the performance is improved by up to 3.3% and 3.7%, respectively, in R-449A and R-454C plants operating in Palermo. Finally, the use of LL-SLHX slightly reduces the sCOP worsening when passing from cold to hot climates.

Table 8 reports the subdivision of the energy consumptions in terms of MT, LT, and parallel compressors and the condenser fan. For synthetic refrigerants, MT1 and MT2 compressor consumptions are grouped together in MT compressors, while for R-744, the MT and LT compressor refer to the HP and LP compressor, respectively, with reference to Figure 5.

Despite that LT's cooling load is only 30% of the total cooling load, the consumption of LT compressors when operated with synthetic refrigerants is about 50% in all cities and plant configurations, due to the much higher compression ratio shown in Figure 8. On the other hand, R-744 LT compressors consume around 20% of the total energy consumption, without significant differences between the three cities. Indeed, the suction and discharge pressures for LP compressors in CO_2 systems are consistent with the minimum LT and MT pressures, leading to a LP compression ratio of ~2.20 at all ambient temperatures. The

minor differences on the consumptions are attributable to the condenser outlet, which affects the evaporator required mass flow rate and, in turn, compression power.

Table 8. Partition of seasonal energy consumptions for all configurations and fluids analyzed: Milano (MI), Rome (RO), and Palermo (PA).

Configuration and Fluid	Energy Consumption [MWh]											
	MT Compressors			LT Compressors			ParallelCompressors			Fan		
	MI	RO	PA	MI	RO	PA	MI	RO	PA	MI	RO	PA
R-449A Base	147.26	155.95	168.04	142.23	146.84	152.92	-	-	-	9.16	9.26	10.10
R-454C Base	150.53	158.81	170.25	154.17	159.10	166.70	-	-	-	9.16	9.26	10.10
R-449A LL-SLHX	144.29	152.06	162.53	137.09	142.07	147.94	-	-	-	9.16	9.26	10.10
R-454C LL-SLHX	148.18	155.81	165.78	148.15	152.13	158.94	-	-	-	9.16	9.26	10.10
R-744	214.84	229.06	242.90	63.64	64.44	65.27	34.94	38.03	49.89	14.58	14.81	16.87

The parallel compressors in R-744 systems account for 11% of the total energy consumption in Milano and Rome, while in Palermo, they account for more than 13%. The higher the temperature is, the higher the share of parallel compression consumption. This results from the assumption of fixing the separator pressure to a low value (36 bar), which is common in practice but not optimal from a thermodynamic standpoint. It is suggested that future work should assess the R-744 system with a separator pressure optimized for each ambient temperature.

Finally, the fan consumption for synthetic refrigerants is the same between the configurations since a single condenser design was simulated, and it changes slightly with higher consumption with higher ambient air temperature, owing to the fan control logic described in Section 3. It must be noted that the fans of R-744 systems consume more than those of synthetic refrigerants as they were oversized to minimize the refrigerant temperature at the gas cooler outlet.

5. Conclusions

In this paper, a steady-state model for simulating an existing commercial food refrigerating facility using three different refrigerants is developed. A state-of-the-art R-744 system architecture with parallel compression, flash gas bypass, and a suction line–liquid line heat exchanger is compared to both a basic R-454C and R-449A system architecture and one with an internal heat exchanger.

The synthetic refrigerants are first compared between themselves, showing that, due to the lower phase-change enthalpy of R454C with respect to R-449A, to provide the same cooling capacity, a higher mass flow rate is required. This leads to a higher burden on the compressors and, depending on the layout and on the outdoor temperature, to a higher number of active compressors. Moreover, a higher condensing temperature is required to overcome the higher mass flow rate and the higher temperature glide of R-454C.

Then, the results reveal that R-454C and R-449A basic systems have a higher COP than R-744 advanced systems only when the outdoor ambient temperature is higher than 15 °C, while the addition of a LL-SLHX for HFOs-based systems improves performance by 3–4%. In terms of sCOP, the R-744 system performed worse than R-454C and R-449A in all locations. In Milano, the sCOP of the R-744 system is 7% and 13% lower than R-454C and R-449A systems with IHX, respectively; in Rome, 9% and 14%; in Palermo, 12% and 17%.

The study highlights the importance of carefully evaluating all available technologies to design food preservation refrigeration systems that reduce energy consumption and related indirect emissions for climatic conditions.

Future work should assess the studied plants from a TEWI perspective, which requires the charge leakage evaluation for each configuration, to determine whether the superior performance of synthetic refrigerants from the energy efficiency point of view extends also to the environmental point of view.

Author Contributions: Conceptualization, W.F., L.M. and F.C.; methodology, W.F. and L.M.; software, W.F. and L.M.; formal analysis, L.M. and F.C.; resources, F.C.; data curation, W.F.; writing—original draft preparation, F.C. and W.F.; writing—review and editing, L.M.; supervision, L.M.; project administration, F.C. All authors have read and agreed to the published version of the manuscript.

Funding: This research received no external funding.

Data Availability Statement: The original contributions presented in the study are included in the article. Further inquiries can be directed to the corresponding authors.

Acknowledgments: We thank Nippon Gases, Alfa Projekt, and Chemours for their valuable technical support and contribution to the definition and development of the paper. We also extend our gratitude for the ideas shared during the preparation of the conference paper [28] that was the foundation for this work.

Conflicts of Interest: Author Fabrizio Codella is employed by the company Chemours Italy. The remaining authors declare that the research was conducted with the utmost integrity and transparency, in the absence of any commercial or financial pressure that could influence the results and be construed as a potential conflict of interest.

Nomenclature

Symbol	Quantity	Unity of Measurement
A	Area	(m^2)
C	Heat capacity	(W/K)
COP	Coefficient Of Performance	(-)
CR	Capacity Ratio	(-)
GWP	Global Warming Potential	(-)
h	Enthalpy	(J/g)
H_{lg}	Liquid-to-vapor enthalpy	(J/g)
m	Mass flow rate	(g/s)
N	Number of revolutions per minute	(rpm)
NBP	Normal Bubble Point	(K)
NTU	Number of Transfer Units	(-)
o	Hour of the year	(h)
P	Pressure	(Pa)
P_{CRIT}	Critical Pressure	(Pa)
Q	Heat power	(W)
R	Thermal resistance	(K/W)
sCOP	Seasonal Coefficient Of Performance	(-)
T	Temperature	(K)
T_{CRIT}	Critical Temperature	(K)
U	Global heat transfer coefficient	(W/m^2K)
W	Mechanical Power	(W)
W_{TOT}	Total Energy Consumption	(J)
ε	Heat exchanger effectiveness	(-)
β	Compression ratio	(-)

Subscripts		**Acronyms**	
AIR	Air side	HP	High Pressure
AIR, AMB	Ambient Air	IHX	Internal Heat Exchanger
APP	Approach	LL-SLHX	Liquid Line—Suction Line Heat Exchanger
C	Compressor	LP	Low Pressure
COND	Condenser	LT	Low Temperature
DESIGN	Design	MI	Milano
EVA	Evaporator	MT1	Medium Temperature 1
GC	Gas Cooler	MT2	Medium Temperature 2
GL	Glide	PA	Palermo
IN	Inlet	RO	Rome
K	Conductivity	VCC	Vapor Compression Cycle
MAX	Maximum		
MIN	Minimum		
OUT	Outlet		
REF, R	Refrigerant		
SH	Superheat		
SUB	Subcooling		

References

1. UNFCCC/COP. Kyoto Protocol to the United Nations Framework Convention on Climate Change. In Proceedings of the Conference of the Parties, Third Session, Kyoto, Japan, 1–10 December 1997.
2. Paris Agreement on Climate Change. 2015. Available online: https://unfccc.int/process-and-meetings/the-paris-agreement (accessed on 15 October 2024).
3. Calm, J.M. The next Generation of Refrigerants—Historical Review, Considerations, and Outlook. *Int. J. Refrig.* **2008**, *31*, 1123–1133. [CrossRef]
4. Tassou, S.A.; Ge, Y.; Hadawey, A.; Marriott, D. Energy Consumption and Conservation in Food Retailing. *Appl. Therm. Eng.* **2011**, *31*, 147–156. [CrossRef]
5. Coulomb, D. Refrigeration and Cold Chain Serving the Global Food Industry and Creating a Better Future: Two Key IIR Challenges for Improved Health and Environment. *Trends Food Sci. Technol.* **2008**, *19*, 413–417. [CrossRef]
6. Maykot, R.; Weber, G.C.; Maciel, R.A. Using the TEWI Methodology to Evaluate Alternative Refrigeration Technologies. In Proceedings of the International Refrigeration and Air Conditioning Conference, West Lafayette, IN, USA, 12–15 July 2004.
7. UN Environment Programme. Montreal Protocol on Substances That Deplete the Ozone Layer. 1987. Available online: https://ozone.unep.org/treaties/montreal-protocol (accessed on 15 October 2024).
8. Heath, E.A. Amendment to the Montreal Protocol on Substances That Deplete the Ozone Layer (Kigali amendment). *Int. Leg. Mater.* **2017**, *56*, 193–205. [CrossRef]
9. European Union. *Regulation (EU) 2024/573 of the European Parliament and of The Council of 7 February 2024 on Fluorinated Greenhouse Gases, Amending Directive (EU) 2019/1937 and Repealing Regulation (EU) No 517/2014*; European Union: Brussels, Belgium, 2024.
10. Codella, F.; Christmann, J.-M. Low-GWP HFO Refrigerants Proven Benefits: A Retailer Case. 2023. Available online: https://www.centrogalileo.it/xx-european-conference-conclusions/ (accessed on 15 October 2024).
11. Yu, B.; Yang, J.; Wang, D.; Shi, J.; Chen, J. An Updated Review of Recent Advances on Modified Technologies in Transcritical CO_2 Refrigeration Cycle. *Energy* **2019**, *189*, 116147. [CrossRef]
12. Citarella, B.; Viscito, L.; Mochizuki, K.; Mauro, A.W. Multi-Criteria (Thermo-Economic) Optimization and Environmental Analysis of a Food Refrigeration System Working with Low Environmental Impact Refrigerants. *Energy Convers. Manag.* **2022**, *253*, 115152. [CrossRef]
13. Giménez-Prades, P.; Navarro-Esbrí, J.; Udroiu, C.-M.; Mota-Babiloni, A. Influence of Subcooling in R-449A Supermarket Refrigeration System and Screening of Refrigerant Mixtures for Its Energetic and Environmental Improvement. *Appl. Therm. Eng.* **2024**, *236*, 121787. [CrossRef]
14. Devecioğlu, A.G.; Oruç, V. Drop-in Assessment of Plug-in R404A Refrigeration Equipment Using Low-Global Warming Potential Mixtures. *Int. J. Low-Carbon Technol.* **2022**, *17*, 991–999. [CrossRef]
15. Gullo, P.; Elmegaard, B.; Cortella, G. Energy and Environmental Performance Assessment of R744 Booster Supermarket Refrigeration Systems Operating in Warm Climates. *Int. J. Refrig.* **2016**, *64*, 61–79. [CrossRef]
16. Sun, Z.; Li, J.; Liang, Y.; Sun, H.; Liu, S.; Yang, L.; Wang, C.; Dai, B. Performance Assessment of CO_2 Supermarket Refrigeration System in Different Climate Zones of China. *Energy Convers. Manag.* **2020**, *208*, 112572. [CrossRef]

17. Jeon, M.-J.; Lee, J.-H. Thermodynamic Comparative Analysis of Cascade Refrigeration System Pairing R744 with R404A, R448A, and R449A with Internal Heat Exchanger: Part 1—Coefficient of Performance Characteristics. *Energies* **2024**, *17*, 4481. [CrossRef]
18. Lemmon, E.W.; Bell, I.H.; Huber, M.L.; McLinden, M.O. *NIST Standard Reference Database 23: Reference Fluid Thermodynamic and Transport Properties-REFPROP, Version 10.0*; National Institute of Standards and Technology: Gaithersburg, MD, USA, 2018.
19. Ferretto, W.; Molinaroli, L.; Inzoli, F.; De Antonellis, S. Development and Validation of a Model for an Air-to-Air Air Conditioner. *J. Phys. Conf. Ser.* **2024**, *2685*, 012038. [CrossRef]
20. Joppolo, C.M.; Molinaroli, L.; Pasini, A. Numerical Analysis of the Influence of Circuit Arrangement on a Fin-and-Tube Condenser Performance. *Case Stud. Therm. Eng.* **2015**, *6*, 136–146. [CrossRef]
21. Wang, C.-C.; Lee, C.-J.; Chang, C.-T.; Lin, S.-P. Heat Transfer and Friction Correlation for Compact Louvered Fin-and-Tube Heat Exchangers. *Int. J. Heat Mass Transf.* **1999**, *42*, 1945–1956. [CrossRef]
22. Bell, K.J. An Approximate Generalized Design Method for Multicomponent/Partial Condensers. *AIChE Symp. Ser.* **1972**, *69*, 72–79.
23. Gnielinski, V. New Equations for Heat and Mass Transfer in Turbulent Pipe and Channel Flow. *Int. Chem. Eng.* **1976**, *16*, 359–368.
24. Cavallini, A.; Col, D.D.; Doretti, L.; Matkovic, M.; Rossetto, L.; Zilio, C.; Censi, G. Condensation in Horizontal Smooth Tubes: A New Heat Transfer Model for Heat Exchanger Design. *Heat Transf. Eng.* **2006**, *27*, 31–38. [CrossRef]
25. Blasius, H. Das Aehnlichkeitsgesetz Bei Reibungsvorgängen in Flüssigkeiten. In *Mitteilungen über Forschungsarbeiten auf dem Gebiete des Ingenieurwesens*; Springer: Berlin/Heidelberg, Germany, 1913; pp. 1–41.
26. Moreno Quibén, J.; Thome, J.R. Flow Pattern Based Two-Phase Frictional Pressure Drop Model for Horizontal Tubes, Part II: New Phenomenological Model. *Int. J. Heat Fluid Flow* **2007**, *28*, 1060–1072. [CrossRef]
27. Sawalha, S. Theoretical Evaluation of Trans-Critical CO_2 Systems in Supermarket Refrigeration. Part I: Modeling, Simulation and Optimization of Two System Solutions. *Int. J. Refrig.* **2008**, *31*, 516–524. [CrossRef]
28. Ferretto, W.; Molinaroli, L.; Codella, F. Energy Efficiency and System Performance of R-454C, R-449A, and R-744 in Food Retail Refrigeration Systems: A Comparison. In Proceedings of the 8th IIR International Conference on Sustainability and the Cold Chain, Tokyo, Japan, 9–11 June 2024.

Disclaimer/Publisher's Note: The statements, opinions and data contained in all publications are solely those of the individual author(s) and contributor(s) and not of MDPI and/or the editor(s). MDPI and/or the editor(s) disclaim responsibility for any injury to people or property resulting from any ideas, methods, instructions or products referred to in the content.